Indian Journal of Chemistry
Vol. 62, September 2023, pp. 931-939
DOI: 10.56042/ijc.v62i9.2574

Determination of alpha-lipoic acid in pharmaceutical samples using inhibitory kinetic approach in SLS micellar medium

Abhishek Srivastava[a]*, Neetu Srivastava[b] & Ruchi Singh[c]

[a] Department of Chemistry, GLA University, Mathura 281 406, U.P., India

[b] Department of Chemistry, D.D.U. Gorakhpur University, Gorakhpur 273 009, U.P., India

[c] Department of Chemistry, B. N. College of Engineering & Technology, Lucknow 226 201, U.P., India

Email: aabhichem@gla.ac.in

Received 12 January 2023; accepted(revised) 14 August 2023

A novel, repeatable, and swift kinetic approach for determining alpha-lipoic acid (ALA) in sodium lauryl sulfate (SLS) micellar medium has been presented, and it has been connected to ALA determination in drug formulations. The approach is based on ALA inhibitory property. ALA (containing two sulfur atoms) forms a chelate with Pd^{2+}, lowering the effective [Pd(II)], and ultimately, the Pd^{2+}catalyzed cyanide substitution rate from $[Fe(CN)_6]^{4-}$ by 4-cyanopyridine (4-CNpy). Fixed times of 5 and 10 min have been chosen under optimal reaction conditions with [4-CNpy] = 2.0×10^{-3} mole dm^{-3}, *p*H = 3.50 ± 0.02, Temp = 298 ± 0.2 K, I = 0.1 mole dm^{-3} ($NaClO_4$), $[Fe(CN)_6^{4-}] = 1.25 \times 10^{-4}$ mole dm^{-3}, $[Pd^{+2}] = 6.0 \times 10^{-5}$ mole dm^{-3}, and [SLS] = 7.75×10^{-3} mole dm^{-3} to calculate the absorbance at 477 nm associated with the final substitution product $[Fe(CN)_5$ 4-CNpy$]^{3-}$. ALA's inhibiting influence on the Pd^{2+}catalyzed cyanide substitution with 4-CNpy from $[Fe(CN)_6]^{4-}$, has been represented by a modified mechanistic approach. The concentration of ALA in various water specimens can be measured at the micro-level down to 1.0×10^{-6} mole dm^{-3} using the established kinetic spectrophotometric approach. The suggested method is highly reproducible and has been effectively applied to accurately quantify the ALA in pharmaceutical samples. Even as much as 1000 with [ALA], typical additives used in medications do not significantly hinder the determination of ALA.

Keywords: Inhibitory effect, Alpha-lipoic acid, Surfactant medium, Pharmaceutical preparations, Hexacyano ferrate (II), Excipients

The body naturally produces alpha-lipoic acid (ALA), often referred to as thioctic acid (TA), which is necessary for the operation of certain oxidative metabolic enzymes [1, 2]. Its main function is to use oxygen to turn blood sugar (glucose) into energy [3, 4]. ALA is a sulfur-containing short-chain fatty acid (Fig. 1). ALA is a powerful antioxidant with numerous metabolic benefits such as antiobesity, glucose reduction, insulin sensitization, and cholesterol reduction. ALA is biologically significant and possesses anti-inflammatory, detoxifying, neuroprotective, anti-aging, and cardiovascular properties[5-9]. ALA is a good contender for metal detoxification because it can efficiently and selectively bind the majority of divalent metal ions both *in vitro* and *vivovia* different mechanistic pathways to form organometallic complexes. Due to the existence of two sulfur atoms with lone pairs of electrons, ALA can form chelates with metal ions.

Fig. 1 — Structure of alpha lipoic acid

Due to their surface-active characteristics, surfactants are frequently employed in modern industries[10-12]. Surfactants' amphiphilic structure, which includes both a tail (hydrophobic) and head (hydrophilic), is what gives them their surface activity[13]. At modest concentrations, the water-based solution of the surfactant behaves as an electrolyte. Micellization takes place in an aquatic environment because one substrate contains both hydrophilic and hydrophobic components. The critical micelle concentration (CMC) is the typical concentration of surfactant at which micellization initiates automatically[14]. Due to the repulsive and attractive interactions that exist between surfactant molecules, the molecules will self-associate beyond CMC and constitute micelles of different shapes and sizes. At 298 K, the CMC value of the anionic surfactant sodium lauryl sulphate (SLS) ranges from 8.0×10^{-3} M to 8.5×10^{-3} M[15–17]. In comparison to pure

solvents, micelle-bound reactants experience a totally distinct reaction environment. The extent of substrate interaction with the micelle aggregates in a micellar medium determines the reaction rate.

Sulfur has remained the dominant heteroatom for centuries in the wide range of fungicides, insecticides, and bioactive compounds. Organosulfur compounds function specifically as structural proteins and enzymes in various metabolic processes[18-20]. Analytical chemists are constantly sought after by the pharmaceutical sector for the most effective technology for detecting and quantifying sulfur-containing bioactive compounds and medicines in various samples. The basic importance and applicability of the oxidation-reduction/ligand exchange processes of complexes containing transition metals in analytical, organometallic, and synthetic chemistry encouraged a large number of scientists to explore their kinetics [21-24]. Kinetic analyses of the Fe(II) and Co(II) complexes oxidation and metal-catalyzed cyanide substitution from $[Ru/Fe(CN)_6]^{3-}$by nitrogen heterocyclic ligands have been reported by a number of authors [25-27]. The aforementioned processes have also successfully been employed for the trace-level evaluation of catalysts and medications/moieties that have a profound affinity for catalysts[28-30].

Different methods are frequently employed to quantify thio compounds in analytical, biological, and pharmacological materials. The quantification methodology includes potentiometry[31], spectro-photometry[32,33], chromatography[34-36], fluorimetry[37], NMR-spectrometry[38], flow injection analysis[39], colorimetry[29], and voltammetry[40]. The aforementioned techniques may have a number of limitations, including a significant initial investment, a lengthy process, heavy equipment, and an elevated cost for the analysis of samples. A relatively small number of investigations have been conducted using the kinetic approach, which only requires a UV-Visible spectrophotometer to quantify thio compounds[28-30, 41].

Several publications have demonstrated metal-catalyzedAg(I)/Hg(II)/Pd(II), cyanide exchange by heterocyclic ligands containing nitrogen from Fe(II)/Ru(II) cyano complexes[26,27]. The micro-level evaluation of utilized catalysts and medications or compounds with a potent affinity for catalysts has also been effectively accomplished using these reactions[28-30]. Through the formation of a stable complex with Pd^{2+}, organosulfur compounds significantly reduce the catalytic effectiveness of Pd(II), which reduces the exchange of cyanide to a significant extent. This inhibiting property of thio moieties (containing sulfur as S-, -S-, and -SH) can be employed for their quantification at trace levels utilizing the kinetic spectrophotometric approach. ALA (containing two "S") similarly reduces Pd(II) catalytic efficacy, lowering the cyanide exchange rate from $[Fe(CN)_6]^{4-}$ by 4-CNpy. Due to the ALAs' potent inhibitory effect on Pd(II)'s catalytic effectiveness, we developed a straightforward, repeatable, and quick kinetic spectrophotometric technique for the micro-level detection of ALA in various water specimens decreased to 1.0×10^{-6} mole dm^{-3}. The developed procedure has also been used to quickly and accurately quantify ALA in various commercial samples with excellent consistency. The technique can be used to determine numerous medicines and biological substances at trace levels that have the potential to severely reduce Pd(II)'s catalytic efficacy.

Experimental Section

Reagent Used

All chemicals that were utilized were pure and of analytical grade. The stock solution of each reagent was directly prepared by weighing its accurate amount and further dissolving it in double-distilled water. To avoid the potential photo-decomposition of $K_4[Fe(CN)_6].3H_2O$ (Sigma-Aldrich), an amber-colored bottle was used to preserve its stock solution. Alpha-lipoic acid (ALA) and sodium lauryl sulphate were purchased from Himedia and utilized directly. The solution of $PdCl_2$ (Fisher Scientific) was made every day by dissolving its computed amount. $NaClO_4$ (Fisher Scientific) was utilized to control the reaction mixture's ionic strength, while Molechem's NaOH/HCl and potassium hydrogen phthalate was employed for adjusting the reaction medium's *p*H.

Instrumentation

Using a DD LAB (model LAB.PHM.66800620) auto digital *p*H meter, verified with a predefined buffer solution, the *p*H of the reacting solution was monitored. A double-beam UV-Visible spectrophotometer made by Electronics India, model 2375, was deployed for measuring absorbance at 477 nm.

Kinetic Procedure

The absorption values were not modified since, with the exception of the final product, none of the

reacting solutions exhibit significant absorption at the pertinent wavelength. An optimum reaction setting that showed a considerable change in absorbance at 477 nm was carefully chosen from the reaction's extensive kinetic investigation. Due to the limited solubility of ALA in water, its kinetic quantification was performed in SLS micellar medium. Following 30 minutes of thermal equilibration at 298 K, all of the reactive solutions were quickly mixed in the sequence: $PdCl_2$, buffer, SLS, 4-CNpy, $NaClO_4$, and $[Fe(CN)_6]^{4-}$. Immediately following a thorough shaking, the reacting mixture was poured into the spectrophotometric cell. An ingeniously constructed system of circulating water arrangement kept the cell compartment at a constant temperature. The absorbance increase related to the final product was documented. The gradient of the line linking $\log(A_\infty - A_t)$ and time has been employed to calculate the reaction's rate constant (k_{obs}). The quantification of ALA was done using a graph (calibration curve) of absorbance *versus* altering [ALA].

Results and Discussion

The reaction involving 4-CNpy and $[Fe(CN)_6]^{4-}$, which is accelerated by Pd(II), resulting in the final substitution product $[Fe(CN)_5$ 4-CNpy$]^{3-}$. By analyzing the end reaction product's mole ratio and slope ratio, it was determined that the reaction between 4-CNpy and $[Fe(CN)_6]^{4-}$occurs in a 1:1 mole ratio. No modification to the absorption values was made because, with the exception of the ultimate reaction product, none of the reacting solutions displayed any discernible absorption at the examined wavelength. The prominent absorption band at 477 nm corresponds to the finished product $[Fe(CN)_5$ 4-CNpy$]^{3-}$ (spectra not shown).

Optimization of Reaction parameters

Impact of variation of *p*H on substitution rate

The cyanide replacement of $[Fe(CN)_6]^{4-}$ with nitrogen heterocycles, whether catalyzed or uncatalyzed, has been shown to be highly influenced by *p*H[42-43]. By measuring absorbance (after 5, 10, and 15 minutes of reactant mixing) as an indicator of the initial rate at various *p*H levels, the rate of reaction was initially explored in the 2.5 to 7.0 *p*H range. This allowed for the identification of the *p*H value which corresponds to the optimal rate.

The *p*H*versus* absorbance plot (Fig. 2) demonstrates the sluggishness of the reaction at

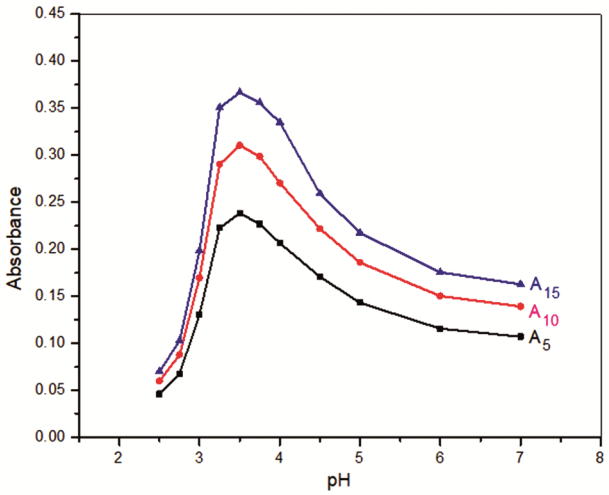

Fig. 2 — Dependence of the absorbanceon *p*H at [4-CNpy] = 2.0×10^{-3} mole dm^{-3}, I = 0.10 mole dm^{-3} ($NaClO_4$), [SLS] = 7.75×10^{-3}mole dm^{-3}, Temp = 298 ± 0.1 K, $[Fe(CN)_6^{4-}] = 1.25 \times 10^{-4}$mole dm^{-3}, and [Pd(II)] = 6.0×10^{-5} mole dm^{-3}

higher $[H^+]$, increases consistently up to *p*H 3.50, and then rapidly declines with subsequent *p*H enhancement up to 7.0. The optimum *p*H value for ALA kinetic quantification might be considered as 3.50. The occurrence of a lesser responsive protonated state of 4-CNpy and $[Fe(CN)_6]^{4-}$($[H_2O(CN)_4Fe(HCN)]^{2-}$) is thought to be the cause of the lowered rate at lesser *p*H. At greater *p*H, 4-CNpy and $[Fe(CN)_6]^{4-}$, appear primarily in their deprotonated state[43,44]. The occurrence of merely a deprotonated version of the 4-CNpyand $[Fe(CN)_6]^{4-}$ accounts for the increment in reaction rate observed in the higher *p*H range. The slower rate at elevated *p*H levels could potentially be related to the reduced H^+ availability required for the catalyst Pd^{2+} to rejuvenate.

Impact of variation of [SLS] on substitution rate

To investigate how [SLS] impacts the substitution rate, every other parameter was kept constant while [SLS] was adjusted from 1.0×10^{-3} mole dm^{-3} to 10.0×10^{-3} mole dm^{-3}. The [SLS] against k_{obs} graph (Fig. 3) demonstrates the increases in reaction rate with [SLS] up to 7.75×10^{-3} mole dm^{-3} (around SLS's CMC) and then remains nearly constant in the examined [SLS] range. At 7.75×10^{-3} M [SLS], the maximum substitution rate was observed; this result is somewhat lower compared to the CMC for previously reported aqueous SLS. SLS's calculated CMC in the studied reaction state is 7.5×10^{-3} mole dm^{-3} which is slightly less compared to the published data in an

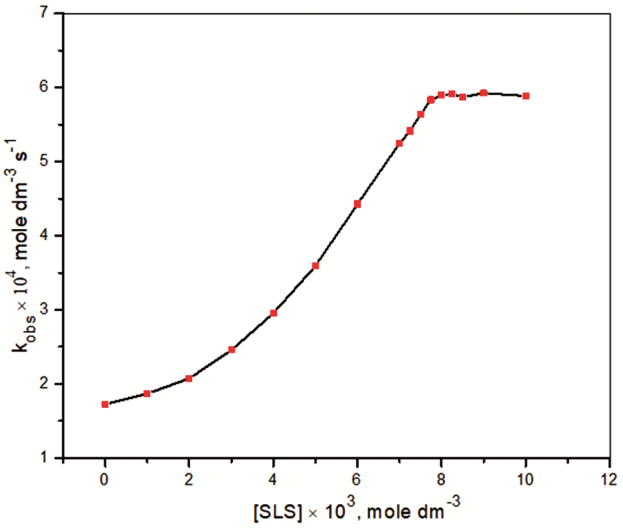

Fig. 3 — Dependence of the rate constant (k_{obs})on [SLS] at [4-CNpy] = 2.0 × 10^{-3} mole dm^{-3}, I = 0.10 mole dm^{-3}($NaClO_4$), *p*H = 3.50 ± 0.02, Temp = 298 ± 0.1 K, $[Fe(CN)_6^{4-}]$ = 1.25 × 10^{-4}mole dm^{-3}, and [Pd (II)] = 6.0 × 10^{-5} mole dm^{-3}

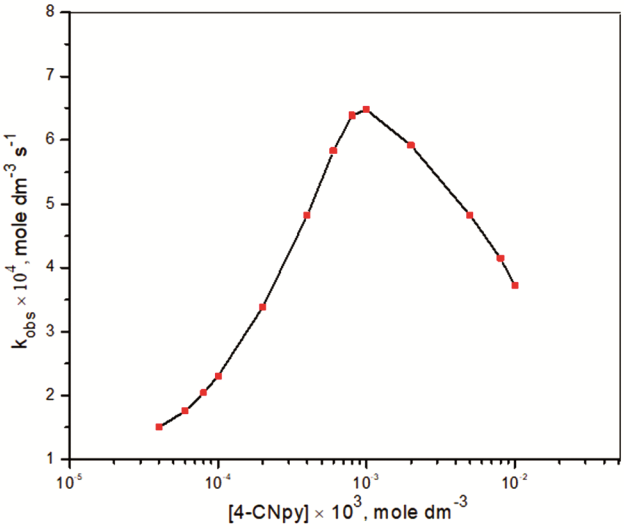

Fig. 4 — Dependence of the rate constant (k_{obs})on [4-CNpy] at [SLS] = 7.75 × 10^{-3} mole dm^{-3}, I = 0.10 mole dm^{-3} ($NaClO_4$), *p*H = 3.50 ± 0.02, Temp = 298 ± 0.1 K, $[Fe(CN)_6^{4-}]$ = 1.25 × 10^{-4}mole dm^{-3}, and [Pd (II)] = 6.0 × 10^{-5} mole dm^{-3}

aquatic environment. This is determined by the junction of the two straight lines in the graph of k_{obs} *versus* [SLS]. The reaction moves roughly 3.4 times faster in SLS micellar media compared to aqueous conditions (Fig. 3), which seems consistent with previous findings on the cyanide substitution from $[Fe(CN)_6]^{4-}$ mediated or catalyzed by micelles[27, 42].

Surfactants' ability to create nano-sized micelles and bringing all reacting species together to guarantee a smooth reaction increases the reaction rate in the SLS medium. Anionic surfactant SLS creates a micelle with an outer layer that is negatively charged. Therefore, anionic species shouldn't get to the substrate and micellar surface in the stern layer [45]. Chemical intuition, however, leads us to conclude that all anionic entities get protonated at lower *p*H and turned neutral. In the acidic media, these neutral entities are capable of interacting with the surfactant *via* ion-dipole interactions and hydrogen bonding[46]. Because of the significantly negative charged micellar exterior, the positively charged Pd^{2+}, H^+, and neutral Fe(II) complex are able to come closer to the reactant molecules (in the stern layer) despite being repelled electrostatically[47]. SLS thus facilitates and accelerates the Pd(II) catalyzed cyanide substitution involving $[Fe(CN)_6]^{4-}$ and [4-CNpy] in an acidic media. SLS's CMC is observed to be somewhat lower in the examined reaction condition than in the aqueous environment. Electrostatically, the positively charged H^+ and Pd^{2+} molecules will be drawn to the negatively charged SLS molecule. Reduced repulsion between surfactant molecules' negative charge heads brought on by the positively charged H^+ and Pd^{2+} molecules may be responsible for the witnessed drop in SLS CMC[48].

Impact of variation of [4-CNpy] on substitution rate

Under the optimal *p*H, the influence of [4-CNpy] on the substitution rate was examined at 298 K in the 4.0 × 10^{-5} mole dm^{-3} to 1.0 × 10^{-2} mole dm^{-3} range. The k_{obs} *versus* [4-CNpy] graph (Fig. 4) demonstrate that the substitution rate advances smoothly up to 8.0 × 10^{-4} mole dm^{-3} [4-CNpy] and then roughly stays the same between 8.0 × 10^{-4} and 1.0 × 10^{-3} mole dm^{-3} [4-CNpy]. Then, with additional advancement in [4-CNpy], it drops off dramatically up to 1.0 × 10^{-2} mole dm^{-3} [4-CNpy]. The concentration of CN^- in the reaction mixture will increase with increasing [4-CNpy] *via* the release of CN^- from $[Fe(CN)_6]^{4-}$. The diminished rate at elevated [4-CNpy] may be attributed to the reduced effective concentration of Pd^{2+} through the formation of the complex between Pd^{2+} and CN^-. The decrease in the reaction rate at greater [4CNpy] is caused by the diminished efficiency of catalyst Pd^{2+}.

Impact of variation of $[Fe(CN)_6^{4-}]$ on oxidation rate

Under the optimum conditions of [4-CNpy] and *p*H, while fixing the rest reaction variables, the rate constant was calculated with reference to

$[Fe(CN)_6^{4-}]$in the concentration band of 1.0×10^{-4} mole dm^{-3} to 16.0×10^{-4} mole dm^{-3}. According to the computed rate constant (k_{obs}) for each $[Fe(CN)_6^{4-}]$, exhibited by Fig. 5, it is clear that the examined $[Fe(CN)_6^{4-}]$ range displayed varying order kinetics. The reaction follows first-order kinetics at a lower concentration of $[Fe(CN)_6]^{4-}$, while the order declines from unity when $[Fe(CN)_6^{4-}]$ is greater than 7.25×10^{-4} mole dm^{-3}.

Impact of variation of [Electrolyte] on substitution rate

Ionic strength's effect on substitution rate will be examined by altering the concentration of neutral electrolyte ($NaClO_4$) in the 0.025 mole dm^{-3} to 0.40 mole dm^{-3} range. The other variables of the reaction were maintained at $[Pd(II)] = 6.0 \times 10^{-5}$ mole dm^{-3}, [4-CNpy] = 2.0×10^{-3} mole dm^{-3}, Temp. = 298 ± 0.1 K, [SLS] = 7.75×10^{-3} mole dm^{-3}, $[Fe(CN)_6^{4-}]$ = 1.25×10^{-4} mole dm^{-3}, and *p*H = 3.50 ± 0.02. A negative salt effect could be seen on the graph plotted between k_{obs} *versus* ionic strength (I) (Fig. 6).

Impact of variation of temperature on substitution rate

Under the optimum reaction conditions, as anticipated, the increases in substitution rate were observed when the temperature increased (293 to 313 K). To ensure a minimum probability of product degradation, the temperature range was selected. The reaction proceeds uniformly at a modest pace at 298 K, hence this temperature was preferred for the kinetic investigation. The Arrhenius equation was exploited to calculate the E_a and $\Delta H^{\#}$ values which are 25.59 k J $mole^{-1}$, and 23.11 k J $mole^{-1}$ respectively.

Impact of variation of [Pd(II)] on substitution rate

As Pd(II) catalyzed substitution reaction could eventually be employed to measure Pd(II) at trace levels, it is imperative to investigate the impact of [Pd(II)] on reaction rate. Under the optimum reaction conditions, the rate of reaction was investigated in the 4.0×10^{-7} mole dm^{-3} to 4.0×10^{-3} mole dm^{-3} [Pd(II)] range by measuring absorbance (5, 10, and 15 minutes after reactant mixing) as an indicator of the initial rate at various [Pd(II)] levels. A linear relation was noticed between $[Pd^{2+}]$ and absorbance at low concentrations of Pd(II). The absorbance/reaction rate advances nonlinearly until the concentrations of the iron complex and catalyst become comparable(Fig. 7). The binuclear adduct produced by Pd(II) and $[Fe(CN)_6]^{4-}$ may be the

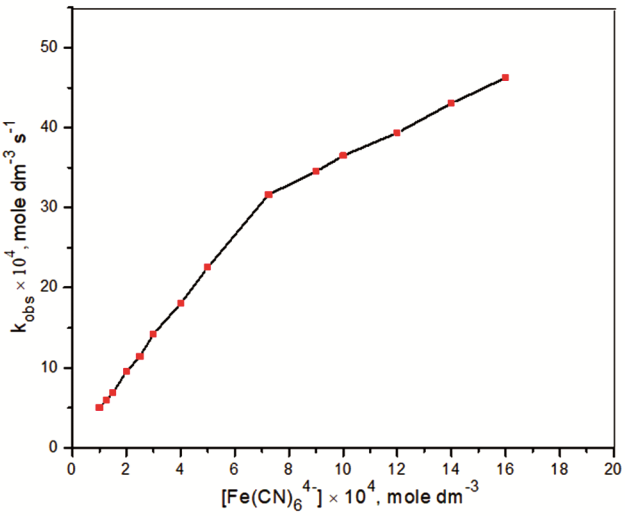

Fig. 5 — Dependence of the rate constant (k_{obs})on $[Fe(CN)_6^{4-}]$ [4-CNpy] = 2.0×10^{-3} mole dm^{-3}, *p*H = 3.50 ± 0.02, Temp = 298 ± 0.1 K, I = 0.10 mole dm^{-3} ($NaClO_4$), [Pd (II)] = 6.0×10^{-5} mole dm^{-3}, and [SLS] = 7.75×10^{-3}mole dm^{-3}

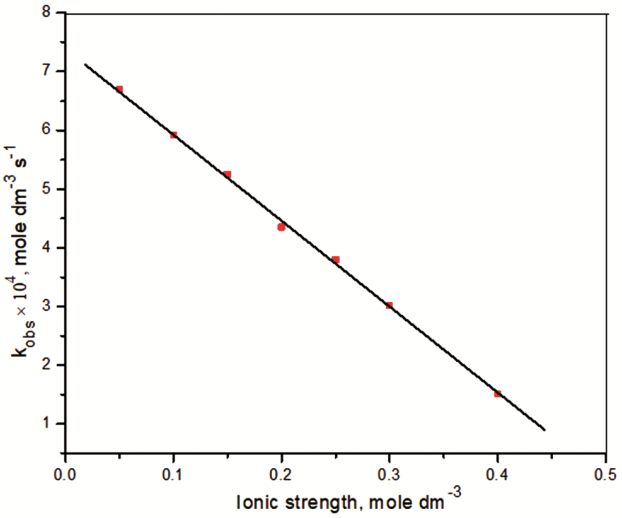

Fig. 6 — Dependence of the rate constant (k_{obs})on [Electrolyte] [4-CNpy] = 2.0×10^{-3} mole dm^{-3}, *p*H = 3.50 ± 0.02, Temp = 298 ± 0.1 K, $[Fe(CN)_6^{4-}]$ = 1.25×10^{-4}mole dm^{-3}, [SLS] = 7.75×10^{-4}mole dm^{-3}, and [Pd (II)] = 6.0×10^{-5} mole dm^{-3}

cause of the acceleration of the reaction rate up to 6.0×10^{-4} mole dm^{-3} $[Pd(II)]$[42]. The resultant binuclear adduct quickly isomerizes in an aqueous solution and produces catalyst as $PdCN^+$ and more labile $[Fe(CN)_5H_2O]^{3-}$.In comparison with $[Fe(CN)_6]^{4-}$, the resulting aqua complex ($[Fe(CN)_5H_2O]^{3-}$) will exhibit more rapid cyanide substitution. Higher $[Pd^{2+}]$ causes more complexation between $[Fe(CN)_6]^{4-}$ and $PdCl_2$, which lowers the catalyst's effective concentration, which ultimately causes a sharp decrease in the substitution rate.

Kinetic quantification of alpha-lipoic acid (ALA)

The prior research on acetylcysteine, thioglycolic acid, D-penicillamine, and other compounds that include sulfur acknowledges that the cyanide substitution rate from $[Fe(CN)_6]^{4-}$ by nitrogen heterocyclic ligands, accelerated by Hg(II) is reduced by the sulfur compounds[28-30]. The effective concentration of Hg(II) decreases due to the stable complex formation between the Hg(II) and added sulfur compounds, which ultimately leads to a slower reaction rate. By the same token, ALAs (containing two sulfur atoms) also forms a chelate with Pd^{2+}, lowering the effective [Pd(II)], and ultimately, the substitution rate. At a set period (5 and 10 minutes after reactant mixing), the absorbance (A_t), associated with the finished substitution product $[Fe(CN)_5$ 4-CNpy$]^{3-}$, with altering [ALA], was documented. ALA was quantified using absorbance against [ALA] plot (calibration curve) that was found linear in the 1.0×10^{-6} to 6.0×10^{-5} mole dm^{-3}ALA concentration band (Fig. 8). Eqs. (1)and(2) express the regression line linking A_t and [ALA].

$$A_5 = 0.2020 - 2.92 \times 10^3[ALA] \quad \ldots(1)$$

$$A_{10} = 0.2750 - 3.64 \times 10^3[ALA] \quad \ldots(2)$$

For the A_5 and A_{10} plots (At against [ALA]), the computed linear regression coefficient and standard deviation were 0.9993, 0.9992, and 0.0016, 0.0020, respectively. After 5 min of injecting the estimated quantity of ALA into the reaction system, the absorbance was recorded. The amount of recovered ALA, estimated using the calibration curve is documented in Table 1. The recovered ALA validates the method's repeatability and accuracy.

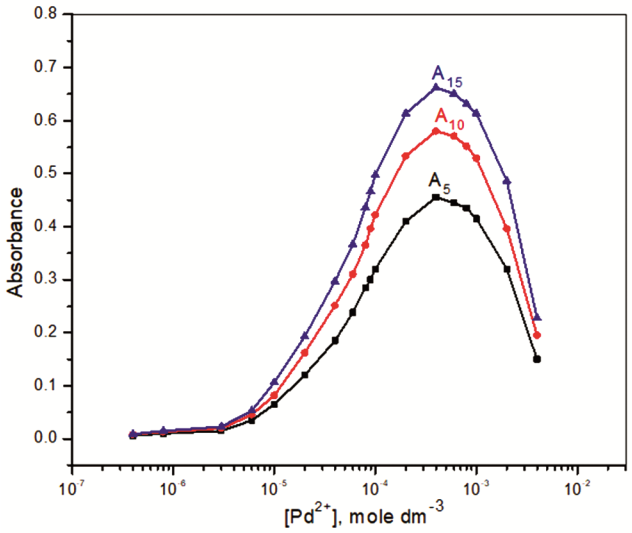

Fig. 7 — Dependence of the absorbanceon [Pd(II)] at I = 0.10 mole dm^{-3}($NaClO_4$), [4-CNpy] = 2.0×10^{-3} mole dm^{-3}, *p*H = 3.50 ± 0.02, Temp = 298 ± 0.1 K, $[Fe(CN)_6^{4-}] = 1.25 \times 10^{-4}$mole dm^{-3}, and [SLS] = 7.75×10^{-4} mole dm^{-3}

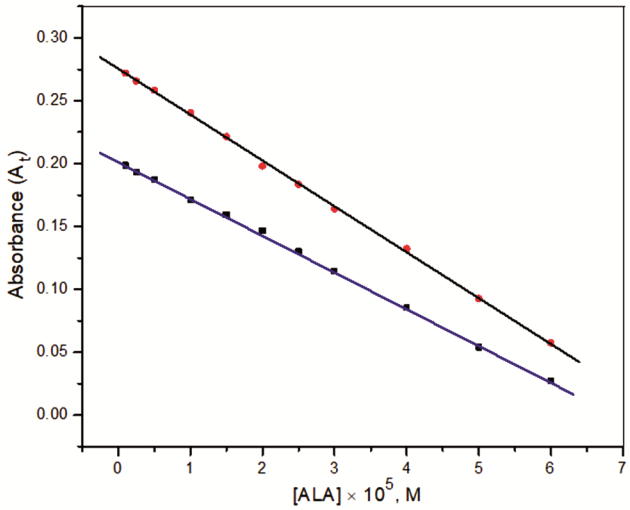

Fig. 8 — Calibration curve for the determination of alpha-lipoic acid at [4-CNpy] = 2.0×10^{-3} mole dm^{-3}, *p*H = 3.50 ± 0.02, Temp = 298 ± 0.1 K, I = 0.10 mole dm^{-3}($NaClO_4$), $[Fe(CN)_6^{4-}] = 1.25 \times 10^{-4}$mole dm^{-3}, [Pd(II)] = 6.0×10^{-5} mole dm^{-3}, and [SLS] = 7.75×10^{-4} mole dm^{-3}

Table 1 — ALA quantification *versus* the added ALA

Experimental Condition: [4-CNpy] = 2.0×10^{-3} mole dm^{-3}, *p*H = 3.50 ± 0.02, Temp = 298 ± 0.1 K, $[Fe(CN)_6^{4-}] = 1.25 \times 10^{-4}$mole dm^{-3}, I = 0.10 mole dm^{-3}($NaClO_4$), [Pd(II)] = 6.0×10^{-5} mole dm^{-3}, and [SLS] = 7.75×10^{-4} mole dm^{-3}

[ALA]×10^{5}mole dm^{-3} (Taken)	A_5		A_{10}	
	[ALA]×10^{5}mole dm^{-3} (Found)	Error	[ALA]×10^{5}mole dm^{-3} (Found)	Error
0.40	0.41 ± 0.025	+ 0.025	0.38 ± 0.046	− 0.050
0.60	0.58 ± 0.018	− 0.033	0.60 ± 0.051	0.000
1.35	1.35 ± 0.031	0.000	1.37 ± 0.068	+ 0.015
1.75	1.78 ± 0.082	+ 0.017	1.71 ± 0.064	− 0.023
2.25	2.29 ± 0.059	+ 0.018	2.28 ± 0.082	+ 0.013
3.00	2.94 ± 0.047	− 0.02	3.00 ± 0.074	0.000
3.75	3.71 ± 0.082	− 0.011	3.78 ± 0.066	+ 0.008
4.50	4.56 ± 0.063	+ 0.013	4.46 ± 0.049	− 0.009

Table 2 — Results of ALA recovery in the presence of neutral additives
Experimental Condition: [4-CNpy] = 2.0×10^{-3} mole dm^{-3}, *p*H = 3.50 ± 0.02, Temp = 298 ± 0.1 K, [$Fe(CN)_6^{4-}$] = 1.25×10^{-4}mole dm^{-3}, [ALA] = 2.0×10^{-5}mole dm^{-3}, I = 0.10 mole dm^{-3}($NaClO_4$), [Pd(II)] = 6.0×10^{-5} mole dm^{-3}, and [SLS] = 7.75×10^{-4} mole dm^{-3}

Excipients	[Excipients] / [ALA]	Recovery ± sd (%)
Maltitol	1000	99.4 ± 0.8
Sorbitol	500	101.0 ± 0.6
Citrate	1000	99.9 ± 0.3
Sucrose	500	100.6 ± 0.7
Magnesium stearate	1000	100.6 ± 0.4
Lactose	500	100.4 ± 0.9
Gelatin	1000	99.7 ± 0.8

Table 3 — Comparison of ALA determination in drug samples with the approved method
Experimental Condition: [4-CNpy] = 2.0×10^{-3} mole dm^{-3}, *p*H = 3.50 ± 0.02, Temp = 298 ± 0.1 K, [$Fe(CN)_6^{4-}$] = 1.25×10^{-4}mole dm^{-3}, I = 0.10 mole dm^{-3}($NaClO_4$), [Pd(II)] = 6.0×10^{-5} mole dm^{-3}, and [SLS] = 7.75×10^{-4} mole dm^{-3}

Samples of Medicine	Recommended Methodology [Recovery ± SD (%)]	Approved Methodology [Recovery ± SD (%)]
Alafin 600 mg Tablet (Fourrts Labs Pvt. Ltd, Chennai, India)	99.79 ± 0.52	99.82 ± 0.46
Alpha Lipoic Acid 300 mg Tablet (Bliss Lifescience LLP, Indore, India)	101.21 ± 0.63	99.41 ± 0.26
Liplac 600 mg Tablet (Apco Pharm Ltd, New Delhi, India)	100.51 ± 0.31	100.21 ± 0.62
Alpha Lipoic Acid 300 mg Capsule (Medizen Labs Pvt. Ltd, Bengaluru, India)	100.67 ± 0.39	99.69 ± 0.48
Alpha Lipoic Acid 350 mg Capsule (Pharmagenica Healthcare Pvt. Ltd, Bengaluru, India)	99.82 ± 0.29	100.35 ± 0.55

A modified mechanistic approach (equations 3–7) established ALA's inhibitory influence on Pd^{2+} accelerated cyanide substitution from $[Fe(CN)_6]^{4-}$ by 4-CNpy. The hypothesized mechanism is similar to the enzyme-catalyzed process in the presence of an inhibitor.

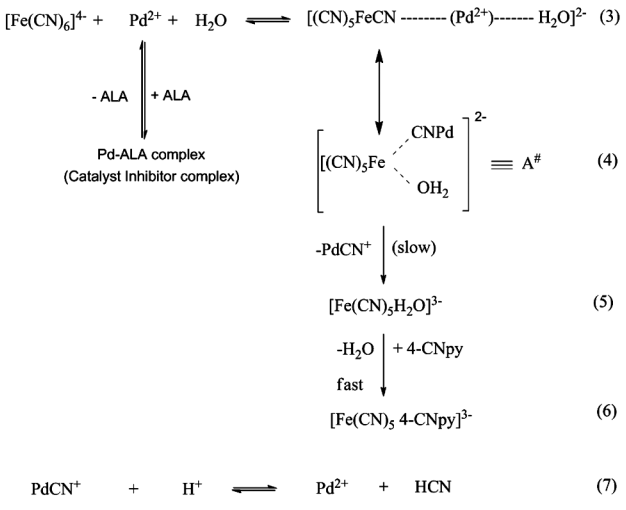

Interference caused by competing constituents

Excipients are inert substances used in drug formulations as fillers, coloring agents, and preservatives in addition to the active medicinal component. Recovery tests were carried out under optimized reaction conditions utilizing the A_5 calibration line, comprising 4.0 μgml^{-1} ALA and a variety of different excipients to examine the impact of excipients. The recovery findings demonstrate that regular additives included in medications do not significantly hinder the quantification of ALA, even when multiplied by 1,000 (Table 2).

Application in medicinal formulations

By using the recommended kinetic spectrophotometric approach, the powdered amount of 8 capsules or tablets was dissolved in 100 ml of water to determine the amount of ALA within different medication samples. The resulting solution was then sonicated for 20 minutes, filtered through Whatman filter paper, and diluted to attain the drug concentration into the A_5 calibrating range. The recommended kinetic approach for the measurement of ALA was used for five distinct medications obtained from local pharmacies that only contained ALA and excipients. The outcome has been compared with the approved method (Table 3). The statistical analysis and average recovery (99-101) findings show that, the suggested methodology for the ALA

determination in pharmaceuticals and water samples is reproducible and accurate[49].

Conclusion

For the quantitative determination of ALA, a novel, swift, and consistently repeatable kinetic approach that relies on the inhibitory behavior of the sulfur-containing molecule ALA towards Pd^{2+} has been presented. Even up to 1000 times with [ALA], the general additives used in medications do not significantly hinder the detection of ALA. The suggested kinetic spectrophotometric approach allows for the micro-level measurement of ALA in various water specimens down to 1.0×10^{-6} mole dm^{-3}. The optimized methodology was also used to quickly quantify ALA in pharmaceutical samples. The suggested methodology for the determination of ALA in water samples and different drugs is reproducible and accurate, as shown by average recovery (99-101%) and statistical analysis results.

Financial Support and Sponsorship:

We did not receive any specific grant for this research from any funding agencies in the public, commercial, or not-for-profit sectors.

Conflicts of interest/Competing interests

None of the authors has any potential or actual conflict of interest to disclose in relation to the published article.

References

1 Tripathi A K, Ray A K, Mishra S K, Bishen S M, Mishra H & Khurana A, *Rev Bras Farmacogn,* 33 (2023) 272.
2 Attia M, Essa E A, Zaki R M & Elkordy A A, *Antioxidants,* 9 (2020) 359.
3 Diane A, Mahmoud N, Bensmail I, Khattab N, Abunada H A & Dehbi M, *Sci Rep,* 24 (2020) 20482.
4 Genazzani A D, Shefer K, Della Casa D, Prati A, Napolitano A, Manzo A, Despini G & Simoncini T, *J Endocrinol Invest,* 41 (2018) 583.
5 Carrier B & Rideout T C, *J Hum Nutr Food Sci,* 1 (2013) 1008.
6 Choi K, Kim J & Kim H, *J Neurol Sci,* 333 (2013) e195.
7 Di Tucci C, Di Feliciantonio M, Vena F, Capone C, Schiavi M C, Pietrangeli D, Muzii L & Benedetti Panici P, *Gynecol Endocrinol,* 34 (2018) 729.
8 Emir D F, Ozturan I U & Yilmaz S, *Am J Emerg Med,* 36 (2018) 1125–e3. https://doi.org/10.1016/j.ajem.2018.03.022
9 Namazi N, Larijani B & Azadbakht L, *Clin Nutr,* 37 (2017) 419.
10 Das B, Kumar B & Begum W, *Chem Africa,* 5 (2022) 459.
11 Zahed M A, Matinvafa M A & Azari A, *Discov Water,* 5 (2022) 2.
12 Mohanambigai D C & Jenif D, *SPAST Abstracts,* 1 (2021) 1.
13 Karimi M A, Mozaheb M A & Hatefi-Mehrjardi A, *J Anal Sci Technol,* 6 (2015) 1.
14 Shah S, Chatterjee S K & Bhattarai A, *J Surfactants Deterg, 19 (2016)* 201.
15 Motin A, Hafiz Mia M A & Nasimul Islam A K M, *J Saudi Chem Soc,* 19 (2015) 172.
16 Mukerjee P, *J Phys Chem,* 76 (1972) 565.
17 Rauf A, Baloch M K, Khan A, Khan Z & Rauf S, *J Chil Chem Soc,* 61 (2016) 3013.
18 Tang K, *Front Mar Sci,* 7 (2020) 68.
19 Abadie C & Tcherkez G, *Commun Biol,* 2 (2019) 379. (https://www.nature.com/articles/s42003-019-0616-y).
20 Kolluru G K, Shen X & Kevil C G, *Arterioscler Thromb Vasc Biol,* 40 (2020) 874.
21 Naik R M, Srivastava A & Asthana A, *J Iran Chem Soc,* 5 (2008) 29.
22 Iioka T, Takahashi S,Yoshida Y, Matsumura Y, Hiraoka S & Sato H, *J Comput Chem,* 40 (2019) 279.
23 Naik R M, Srivastava A, Verma A K, Yadav S B S, Singh R & Prasad S, *Bioinorg Reac Mech,* 6 (2007) 185.
24 Srivastava A, Sharma V, Prajapati A, Srivastava N & Naik R M, *Chem Chem Technol,* 13 (2019) 275.
25 Prasad S, Naik R M & Srivastava A, *Spectrochim Acta A,* 70 (2008) 958.
26 Rastogi R, Srivastava A & Naik R M, *J Disp Sci Tech,* 41 (2020) 1045.
27 Srivastava A, Naik R M & Rastogi R, *J Iran Chem Soc,* 17 (2020) 2327.
28 Srivastava A, Srivastava N, Srivastava K, Naik R M & Srivastava A, *Russ J Phy Chem A,* 96 (2022) 3082.
29 Srivastava A, Sharma V, Singh V K & Srivastava K, *J Mex Chem Soc,* 66 (2022) 57.
30 Srivastava A & Srivastava K, *Phy Chem Res,* 10 (2022) 283.
31 Kyriacou D, *Nature,* 211 (1966) 519.
32 Nugrahani I, Abotbina I M, Apsari C N, Kartavinata T G & Oktaviary R S, *Biointerface Res Appl Chem,* 10 (2019) 4780.
33 Feng G, Sun S, Wang M, Zhao Q, Liu L, Hashi Y & Jia R, *J Water Supply Res T,* 67 (2018) 498.
34 Mohamed W, El-Brashy A, Mohammed M & Amina A, *Acta Chim Slov,* 51 (2004) 283.
35 Dhanure S, Savalia A, More P, Shirode P, Kapse K & Shah V, *Sci Pharm,* 82 (2014) 765.
36 Megoulas N C & Koupparis M A, *J Chromatogr A*, 1026 (2004) 167.
37 Argekar A P, Raj S V & Kapadia S U, *Anal Lett,* 30 (1997) 821.
38 Chao Q, Sheng H, Cheng X & Ren T, *Ana Sci, 21 (2005)* 721.
39 Agrawal G P & Maheshwari R K, *Curr Pharm Anal,* 16 (2020) 487.
40 El-BrashyA M & Al-Ghannam S M, *Microchemical J,* 53 (1996) 420.
41 Srivastava A, *Biointerface Res Appl Chem,* 10 (2020) 7152.

42 Srivastava A, Naik R M, Rai J & Kumar I, *J Surfactants Deter,* 26 (2023) 13.
43 Srivastava A, Naik R M, Rai J & Asthana A, *Russ J Phy Chem,* 95 (2021) 2545.
44 Catalan J, Mo O, Perez P & Yanez M*, J Am Chem Soc, 101* (1997) 6520.
45 Acharjee A, Rakshit A, Chowdhury S, Malik S, Barman M K, Ali M A & Saha B, *J Mol Liq,* 277 (2019) 360.
46 Sar P, Ghosh A, Saha R & Saha B, *Res Chem Intermed,* 41 (2015) 5331.
47 Ghosh A, Das P, Saha D, Sar P, Ghosh S K & Saha B, *Res Chem Intermed,* 42 (2016) 2619.
48 Jimenez R, Bueno E, Cano I & Corbacho E, *Int J Chem Kinet,* 26 (2004) 627.
49 U.S. Pharmacopoeia, 27 (2007) 3338.